Earth and Planetary Science Letters 351–352 (2012) 95–104

Contents lists available at SciVerse ScienceDirect

Earth and Planetary Science Letters

journal homepage: www.elsevier.com/locate/epsl

A mid-Holocene thermal maximum at the end of the African Humid Period

Melissa A. Berke [a,*], Thomas C. Johnson [a], Josef P. Werne [b], Stefan Schouten [c], Jaap S. Sinninghe Damsté [c]

[a] Large Lakes Observatory and Department of Geological Sciences, University of Minnesota Duluth, Duluth, MN 55812, USA
[b] Large Lakes Observatory and Department of Chemistry & Biochemistry, University of Minnesota Duluth, Duluth, MN 55812, USA
[c] NIOZ Royal Netherlands Institute for Sea Research, Department of Marine Organic Biogeochemistry, P.O. Box 59, Den Burg, 1790 AB, Netherlands

ARTICLE INFO

Article history:
Received 14 December 2011
Received in revised form
2 July 2012
Accepted 3 July 2012
Editor: J. Lynch-Stieglitz
Available online 29 August 2012

Keywords:
Holocene
paleotemperature
African Humid Period
Lake Turkana

ABSTRACT

The termination of the African Humid Period (AHP) about 5 thousand years ago (ka) was the most dramatic climate shift in northern and equatorial Africa since the end of the Pleistocene. Based on TEX_{86} paleotemperature data from Lake Turkana, Kenya, we show that a temperature shift of 2–4 °C occurred over the two millennia spanning the end of the AHP, with the warmest conditions occurring at ~5 ka. We note a similar shift, though of a smaller magnitude, in other East African temperature records from Lakes Malawi and Tanganyika, as well as Mt. Kilimanjaro. Additionally, we document the temperature history for the last 220 years from Lake Turkana that indicates the thermal anomaly at 5 ka was warmer than the present day Lake Turkana temperatures and on par with modern temperatures of Lakes Tanganyika and Malawi. We suggest that the thermal response at the end of the AHP may be linked to local insolation during September–November, when local air temperature rises to an annual maximum over Lakes Malawi and Tanganyika and a secondary maximum over Lake Turkana and Mt. Kilimanjaro. September–November insolation peaked at ~5 ka and likely caused air and water temperatures in the region to rise to maxima at that time.

1. Introduction

The precise timing, pace and extent of the African Humid Period (AHP) are the focus of continued investigation, particularly the rate at which much of northern and equatorial Africa changed from a wet, verdant landscape, with a lake-filled "green Sahara" and high lake levels as far south as Lake Rukwa (~8 °S latitude) to expansive desert, diminished lake levels, and the replacement of mesic with drought-tolerant plants. The AHP lasted from ~14.5 to 5 ka, and is attributed to a non-linear response to Northern Hemisphere summer insolation forcing that first strengthened, then weakened the African Monsoon system, amplified by atmosphere-vegetation feedbacks (Kutzbach and Street-Perrott, 1985; Claussen and Gayler, 1997; Liu et al., 2007; Tierney et al., 2011). The environmental response at the end of the AHP, with its abrupt, seemingly geographically extensive character, has been likened to other dramatic wide-spread environmental events, such as the Younger Dryas (deMenocal et al., 2000). However, the climate signal of the AHP appears somewhat spatially and temporally variable across Africa, so the term "African Humid Period," applies neither to the entire continent, nor is its duration fixed within the part of the continent where it does apply. Consequently, understanding the environmental shift at the end of the AHP has been confounded by responses captured in paleorecords, with evidence for both an abrupt shift towards aridity, completed over decades to centuries, and for a more gradual response over several millennia (Niedermeyer et al., 2010; Vincens et al., 2010). While the AHP is reported to have terminated abruptly at 5.5 ka based on changes in dust concentration in ocean sediment core records off northwest Africa (deMenocal et al., 2000), the actual shift to more arid conditions appears to have been latitudinally time transgressive across much of northern Africa (Kuper and Kropelin, 2006).

The thermal evolution during the termination of the AHP is not well documented, partly because of a lack of suitable temperature proxy records. Recently, however, a number of African lake temperature records have been produced through the application of the TEX_{86} temperature proxy. TEX_{86} is based on the degree of cyclization of membrane lipids from aquatic Thaumarchaeota, previously referred to as Crenarchaeota (Brochier-Armanet et al., 2008), specifically isoprenoid glycerol dialkyl glycerol tetraethers (GDGTs), which are well preserved in marine and lacustrine sediments (Schouten et al., 2002; Kim et al., 2010; Powers et al., 2010). The distribution of these compounds correlates with surface water temperature in the oceans and some lakes, and thereby provides the opportunity to reconstruct past temperature (Schouten et al., 2002; Kim et al., 2010; Powers et al., 2010). In many lakes, TEX_{86} may not be a reliable proxy for past temperature, particularly in small lakes where substantial amounts of

* Corresponding author. Present address: Global Change and Ecosystem Center, University of Utah, Salt Lake City, UT 84112, USA.
E-mail addresses: berk0135@umn.edu, melissa.berke@utah.edu (M.A. Berke).

0012-821X/$ - see front matter © 2012 Elsevier B.V. All rights reserved.
http://dx.doi.org/10.1016/j.epsl.2012.07.008

soil-derived isoprenoid tetraether compounds confound the signal derived from aquatic Thaumarchaeota (Blaga et al., 2009; Powers et al., 2010). This terrestrial influence is quantified by the so-called BIT (Branched and Isoprenoid Tetraether) index, a ratio of predominantly soil-derived branched GDGTs to isoprenoid GDGTs produced by aquatic Thaumarchaeota. The BIT index ranges from 0 (predominantly aquatic) to 1 (predominantly terrestrial) (Hopmans et al., 2004). TEX_{86} is not considered to be a reliable recorder of past temperature in lake sediment when BIT values exceed ~0.4 (Blaga et al., 2009). Additionally, the relative distribution of GDGTs can be biased by the presence of methanogenic Euryarchaeota, which generate some of the same membrane lipids as Thaumarchaeota but lack the appropriate temperature relationship (Schouten et al., 2007b). GDGT-0 is a commonly found membrane lipid of Archaea, while crenarchaeol is thought to provide more specific evidence of Thaumarchaeota (Sinninghe Damsté et al., 2002; Pitcher et al., 2011). Thus, a ratio of GDGT-0 to crenarchaeol can be used to assess the influence of methanogenesis, and should be low (<2) for sediments with low methanogenic input (Schouten et al., 2002; Blaga et al., 2009). The TEX_{86} proxy has been applied to several African lake systems, such as Malawi and Tanganyika, and shown to record known climate events such as glacial–interglacial cycles (Powers et al., 2005; Tierney et al., 2008; Woltering et al., 2011) and the Younger Dryas (Powers et al., 2005).

We generated a lake temperature record from Lake Turkana using this TEX_{86} paleothermometer, which shows, in combination with other records, that much of tropical East Africa experienced a significant shift in temperature over the two millennia centered on 5 ka, which undoubtedly added to the stress imposed on the fauna and flora from hydrological changes associated with the end of the AHP.

2. Regional setting and modern climatology

Lake Turkana (3°35′N, 36°7′E) lies in a broad depression at 360 m above sea level between the Ethiopian Rift to the northeast and the Kenyan Rift to the south and is the largest lake in the eastern arm of the Rift Valley, with a length of about 250 km and an average width of 30 km (Fig. 1). The Turkana basin is hot and arid, and subject to extended periods of intense diurnal winds. The amplitude of seasonal variability in air temperature and rainfall, while present at Lake Turkana, is subdued compared to the other great lakes of East Africa. Surface water temperatures in Lake Turkana typically range from about 26 °C to 30 °C throughout the year, while bottom water temperatures exhibit only minor seasonal fluctuations between 24.5 °C and 26.5 °C (Ferguson and Harbott, 1982) (Fig. 2). The lake exhibits weak thermal stratification during the spring months, in contrast to more uniform temperature structure due to wind mixing at other times of the year (Ferguson and Harbott, 1982). Daily mean maximum and minimum air temperatures recorded on the western shore of the lake in 1973–1975 were 32.5 °C and 26.0 °C, respectively, and were slightly cooler in the summer months than in the winter, due to the cooling influence of occasional rains and clouds with passage of the African rain belt, associated with the Intertropical Convergence Zone (ITCZ) (Ferguson and Harbott, 1982). Modern Lake Turkana typically exhibits temperatures 1–3 °C warmer in the north basin than in the south due to upwelling in the south basin produced by the predominantly southerly winds (Fig. 2). Mean annual rainfall in the Turkana Depression is about 200 mm yr^{-1} (Nicholson et al., 1988), while the annual evaporation rate is about 2300 mm yr^{-1} (Ferguson and Harbott, 1982). The closed-basin lake receives 80–90% of its fresh water from the Omo River, which drains the Ethiopian Highlands to the north (Fig. 1), where annual rainfall is in the range of 800–1200 mm yr^{-1} (Ferguson and Harbott, 1982). Lake Turkana has a salinity of about 25, dominated by Na^+, HCO_3^-, and Cl^- ions, and a pH averaging 9.1 (Cerling, 1979; Ferguson and Harbott, 1982). A unique aspect of Lake Turkana among the great lakes of the Rift Valley is that its bottom waters are continuously oxygenated due to its average depth of just 35 m and frequent exposure to intense wind.

3. Materials and methods

3.1. Sample collection

We generated a high-resolution (<90 year time step) temperature record spanning the termination of the AHP in East Africa

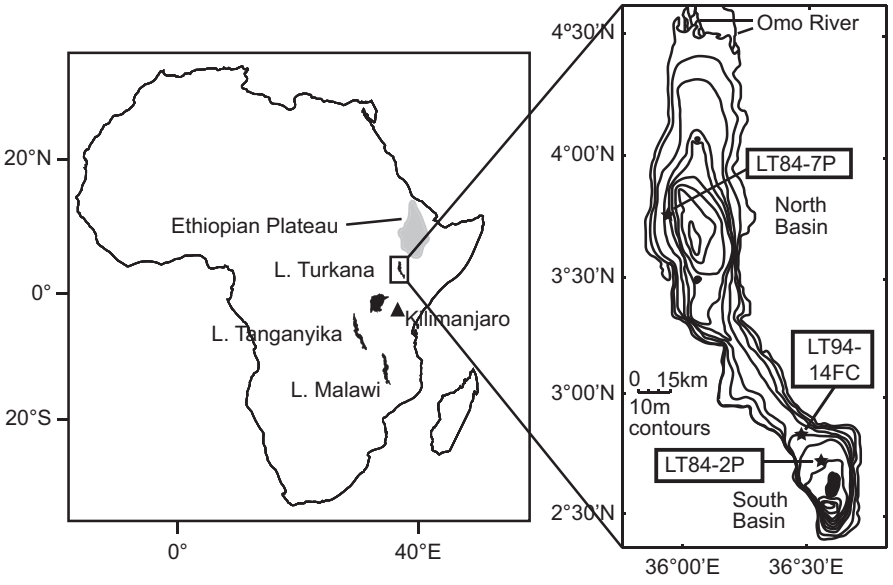

Fig. 1. Map of Africa with Lakes Turkana, Malawi, Tanganyika, and Mt. Kilimanjaro (triangle), and Ethiopian Plateau (shaded), with inset map of Lake Turkana bathymetry and core locations. Bathymetric contours are at 10 m intervals. Two piston cores were chosen for this study, recovered in 57 m of water from the south basin, (LT84-2P) and from 40 m depth in the north basin, (LT84-7P). A freeze core was also used, taken in 38 m of water in the south basin (LT94-14FC).

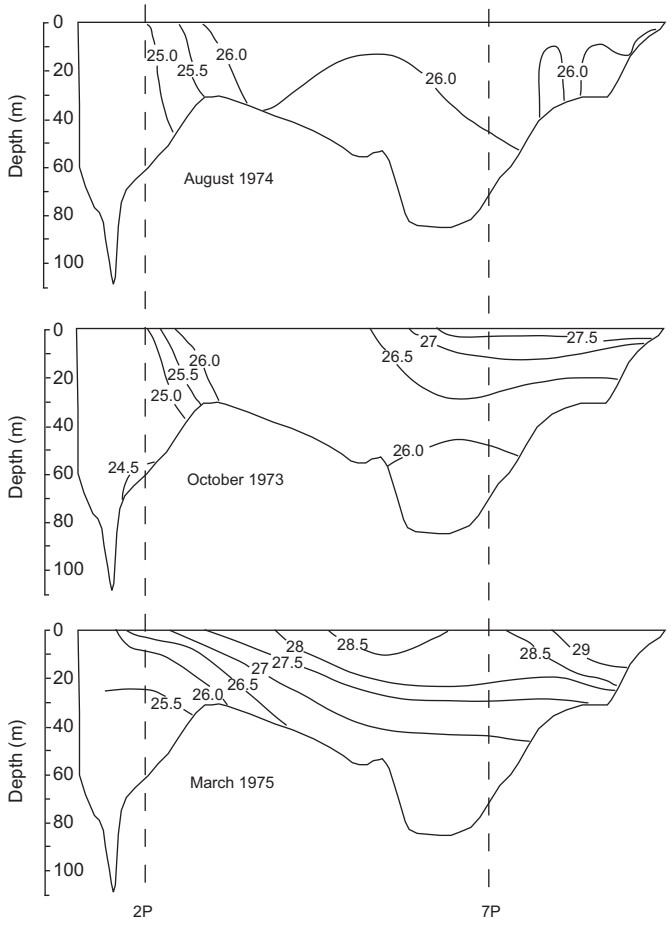

Fig. 2. Temperature structure of Lake Turkana along a north–south transect during August 1974, October 1973 and March 1975 showing a temperature difference between the two basins during each season (~2 °C) and across the annual cycle (Ferguson and Harbott, 1982).

from sediments of Lake Turkana in northern Kenya (Fig. 1) using the TEX_{86} paleotemperature proxy. TEX_{86} values from sediments recovered with Kullenberg piston cores from the south basin (LT84-2P, spanning ~6–1 ka) and the north basin (LT84-7P, spanning ~2.5–0.4 ka), each 12 m long, supplemented by TEX_{86} values from a freeze core recovered from the south basin (LT94-14FC, spanning the interval from AD 1770 to 1990), documenting the more recent temperature history of surface water from Lake Turkana.

3.2. Chronology

Age models for 6 piston cores from Lake Turkana, including LT84-2P and LT84-7P, are published in Halfman et al. (1994). The age models are based on a total of 68 radiocarbon dates, combined with stratigraphic correlations of carbonate abundance ($\%CaCO_3$) and magnetic susceptibility (MS) among the dated cores.

Low abundances of organic carbon in the sediment required the selection of carbonate fractions for dating, including bulk carbonate, ostracods >150 μm, ostracods in the 63–150 μm range, and carbonate <63 μm, which is predominantly euhedral, low-Mg calcite crystals (micrite) 2–5 μm long that precipitates out of the surface waters (Halfman et al., 1994). Ostracods >150 μm consistently provided the youngest dates at any level in the cores (Halfman et al., 1994), while micrite dates tended to be older, presumed to be due to an eolian contribution of fine-grained carbonate from nearby exposed lake deposits. A total of 19 radiocarbon dates were obtained on the various carbonate fractions from LT84-2P, of which three dates were on ostracods greater than 150 μm. We constructed an age model that is based on the 3 dates on the large ostracods in combination with 9 stratigraphic correlations of MS or $\%CaCO_3$ peaks with nearby core LT84-1P that has ostracod dates (>150 μm) at 3 horizons (Fig. 3 and Table S1) (Halfman et al., 1994). The MS and $\%CaCO_3$ peaks were assigned the average of the ages in the two cores by Halfman et al. (1994) by interpolation between radiocarbon-dated horizons. The average difference in age assignments to the respective MS and carbonate horizons in the two cores was 65 years. The resultant age model is defined by the equation:

$$\text{Age(ka)} = 1.120 + 0.00406 \times \text{Depth(cm)}, \quad R^2 = 0.998 \tag{1}$$

The age discrepancy between coarse ostracods and micrite was minor in this core, with the fine fraction estimated to contain only 5% "old" carbon (Halfman et al., 1994). An age model based on a linear regression through all 19 radiocarbon dates in core LT84-2P, independent of stratigraphic correlation to other cores, would be defined by the equation:

$$\text{Age(ka)} = 1.368 + 0.00388 \times \text{Depth(cm)}, \quad R^2 = 0.916 \tag{2}$$

While we employ the first age model, the second one differs from it by a maximum of 248 years at the top of the core and by just 60 years at 10 m burial depth. The age model for core LT84-7P is based on 5 AMS dates on ostracods >150 μm, supplemented by 14 stratigraphic correlations of MS or $\%CaCO_3$ to two dated cores nearby (Fig. 3 and Table S1) (Halfman et al., 1994). It is defined by the equation:

$$\text{Age(ka)} = 0.497 + 0.00163 \times \text{Depth(cm)}, \quad R^2 = 0.966 \tag{3}$$

The extrapolated core–top ages of 1.1 ka for core LT84-2P and 0.5 ka for core LT84-7P are due to over-penetration of the sediment–water interface by the piston corer. This is supported by the observation during coring operations that the top of the piston core weight stand was covered with mud (Halfman et al., 1994), and by post-bomb radiocarbon dates on carbonates in near-surface sediments in three other cores recovered from Lake Turkana. An AMS radiocarbon analysis of ostracods >150 μm from 56 to 58 cm depth in a short "Ligi" core, LT90-19LG, recovered from

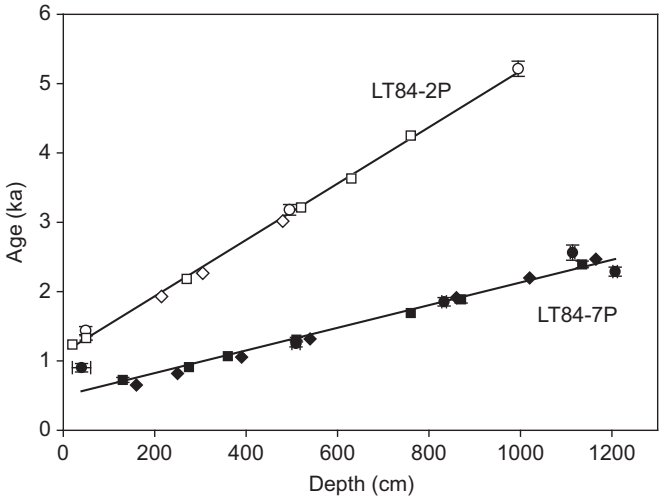

Fig. 3. Lake Turkana age models for LT84-2P, the southern basin core (open symbols) and LT84-7P, the northern basin core (solid symbols). Circles represent calibrated AMS radiocarbon dates on ostracod shells >150 μm, squares represent calibrated carbonate correlation dates, and diamonds represent magnetic susceptibility stratigraphic correlation ages (Halfman et al., 1994). Error bars represent range of depths sampled in the core (horizontal error bars) and $\pm 1\sigma$ radiocarbon error (vertical error bars).

the central basin of Lake Turkana in 1990 by Lister of ETH showed evidence of bomb radiocarbon, with a measurement of 114.8 ± 0.6% modern (AA-8681). No other dates were obtained on this core, but a freeze core, LT90-6FC, recovered near this site had a linear sedimentation rate of about 2 cm/yr, based on ^{210}Pb analyses (Ricketts and Anderson, 1998). Applying this rate to the Ligi core places the actual age of the radiocarbon dated horizon at AD 1962, a time when the atmospheric concentration of radiocarbon was rising too rapidly to ascertain a precise reservoir age for Lake Turkana water. We assume the reservoir age to be zero, but recognize that it could be ~200–300 years, based on the post-bomb measurement.

The age model for LT94-14FC (Ricketts and Anderson, 1998) is based on ^{210}Pb analyses back to AD 1850 and an assumed constant mass accumulation rate prior to this. All radiocarbon dates are presented as calibrated years before 1950 based on the IntCal09 calibration (Reimer et al., 2009) and calculated using CalPal calibration software (Weninger et al., 2011).

3.3. Lipid extraction and analysis

Lipids were extracted from freeze-dried, homogenized sediments using either Soxhlet or accelerated solvent extraction (Dionex™ ASE). The total lipid extract (TLE) was then separated into the neutral, free fatty acid, and phospholipid fatty acid fractions using Alltech Ultra-Clean SPE aminopropylsilyl bond elute columns, cleaned prior to use with 10 mL successive rinses of MeOH followed by 1:1 DCM:2-propanol (v:v). The neutral, free fatty acid, and phospholipid fatty acid fractions were eluted by 8 mL each of 1:1 DCM:2-propanol (v:v), 4% glacial acetic acid in distilled ethyl ether, and MeOH, respectively. Column chromatography using activated alumina was used to further separate the neutral fraction using 9:1 hexane:DCM (v:v) followed by 1:1 DCM:MeOH (v:v), to elute the apolar and polar fractions, respectively. The polar fraction was filtered (0.45 μm PTFE filter) (Hopmans et al., 2000), dried under N_2, then redissolved in 99:1 hexane:isopropanol (v:v) prior to analysis.

GDGTs were analyzed at the Royal Netherlands Institute for Sea Research by high performance liquid chromatography/atmospheric pressure chemical ionization mass spectrometry (HPLC/APCI-MS), using an Agilent 1100 series LC with an Alltech Prevail Cyano column (150 mm × 2.1 mm; 3 μm) (Schouten et al., 2007a). TEX_{86} temperatures were calculated using the ratio of GDGTs I–IV (Schouten et al., 2002). Replicate TEX_{86} analyses indicate a mean reproducibility of ± 0.1 °C for these Lake Turkana records, with a maximum difference of ± 0.2 °C between duplicate analyses. GDGTs were quantified using a C_{46} tetraether lipid as an external standard as described by Huguet et al. (2006).

3.4. Estimation of paleotemperatures using TEX_{86}

An independent calibration of TEX_{86} with surface temperature has been established for lakes (Powers et al., 2004, 2010), with some tropical lake additions (Tierney et al., 2010a). However, TEX_{86} values for Lake Turkana are converted to mean annual lake surface temperatures (LST) using the (sub)tropical relationship for marine sediments, TEX_{86} (high temperature calibration) (Kim et al., 2010). Lake Turkana core–top samples consistently plot anomalously warm on the global lake calibration curve (i.e., the core–top value of TEX_{86} from Lake Turkana is lower than predicted by the global lake calibration curve, given the lake's mean annual lake surface temperature) (Powers et al., 2010), but yield LST similar to those of the present day when using the global marine calibration line (Kim et al., 2010). While this may be due to the slightly brackish composition of Lake Turkana water, indicating the Thaumarchaeota populations here may more closely match those of marine than lacustrine settings, Wuchter et al. (2004) found no influence of salinity on TEX_{86}. Alternatively, we speculate that the calibration offset may result from Lake Turkana having neither a permanent chemocline nor anoxic deep water. Thaumarchaeota are known to be ammonia oxidizers (Konneke et al., 2005; Wuchter et al., 2006), and therefore may be nourished by the proximity of an oxic and anoxic water boundary where turbulent mixing can provide an ample supply of ammonia across the chemocline (Konneke et al., 2005; Blaga et al., 2011). In the absence of such conditions, such as in the oceans and in Lake Turkana, a different community of Thaumarchaea may dominate and generate GDGTs that track the marine TEX_{86} calibration curve. The only other tropical lake that plots as far on the warm side of the global lake calibration curve and fits the marine calibration, Lake Victoria (Powers et al., 2010; Tierney et al., 2010a), also lacks an anoxic hypolimnion, though unlike Lake Turkana, Lake Victoria is not saline. While the selection of the marine calibration curve (Kim et al., 2010) results in absolute values of temperature that are ~4 °C warmer than the lake calibration curve (Powers et al., 2010), the trend of temperature change through time is identical for either the marine or lacustrine calibration (Kim et al., 2010; Powers et al., 2010). The calibration error associated with the marine global calibration dataset based on 255 reconstructed marine temperatures from temperate and tropical settings is ~2.5 °C (Kim et al., 2010), which we believe is a conservative value that exceeds what would be expected within a single large, tropical lake.

3.5. BIT index and GDGT contributions

The BIT values for this study and all lake sediments discussed here were less than 0.3, indicating little impact of soil-derived lipids on the TEX_{86} values (Fig. S1). Similarly, the ratio of GDGT-0/crenarchaeol is < 0.3 for all samples discussed and therefore it is unlikely that there is any substantial methanogenic contributions to the GDGT pool (Blaga et al., 2009) for the Lake Turkana sediments (Fig. S1).

4. Results and discussion

4.1. Lake Turkana climate record trends

Reconstructed temperatures for core LT84-2P in the south basin of Lake Turkana are highly variable throughout the mid-late Holocene, ranging from 23 °C to 28.3 °C (Fig. 4). Lake Turkana waters were coolest ~5.7 ka, and then underwent steady warming of more than 3.5 °C for 8 centuries, culminating in the warmest conditions of the entire record at about 5 ka. The lake experienced subsequent cooling over the following millennium by about 2 °C, and then cooled gradually another ~0.7 °C over the following 3 millennia, but with century-scale fluctuations of ~1 °C superimposed on this slow cooling trend. The north basin temperatures recorded in core LT84-7P fluctuate between ~25.5 °C and 28.3 °C, and display a slight warming trend from 2.5 to 0.5 ka, but with even larger centennial scale fluctuations than in core 2P overlying the longer-term trend (Fig. 4). North basin temperatures are on average ~1.5 °C warmer than the south basin throughout this mid-late Holocene reconstruction. This temperature difference between the basins is consistent with the south-to-north temperature gradient observed in the lake during the stratified conditions today (Fig. 2). This and two additional observations lend credence to the use of TEX_{86} in core 2P as a temperature proxy in Lake Turkana. First, the amplitude of seasonal variability in mean water column temperature is greater in the north basin than in the south (Fig. 2), which may explain

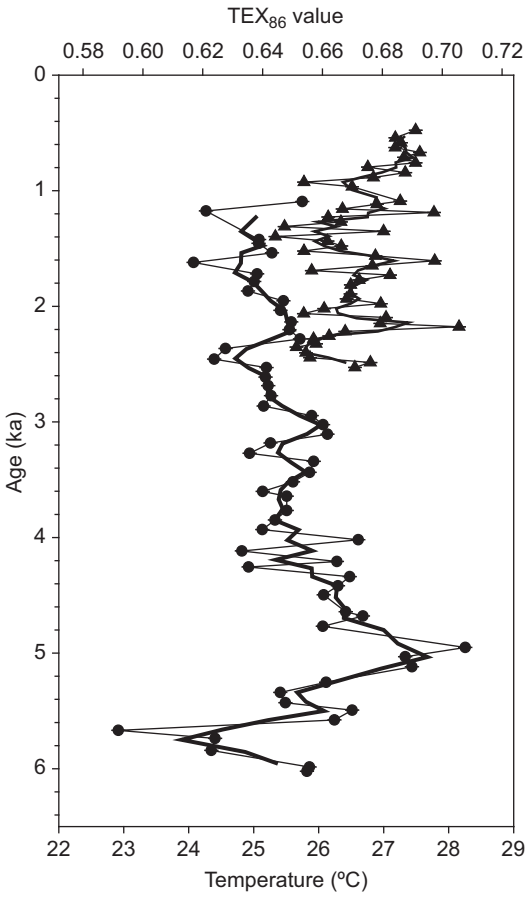

Fig. 4. TEX_{86} records of temperature from the south (circles) and north basins (triangles) of Lake Turkana, with 3-point running averages shown by the heavy lines. Replicate analyses indicate a mean reproducibility of ± 0.1 °C, with a maximum difference of ± 0.2 °C between duplicate analyses.

why there is higher amplitude centennial scale variability in core 7P than in 2P. Second, the lower amplitude of both seasonal and centennial scale variability in temperature in the south basin of the lake makes this the preferred location for recovering a long-term record that is representative of regional temperature change. The north basin temperature profile is not consistently in phase with the south basin record, which likely reflects variable intensity of the wind-driven circulation through time, as reflected on a seasonal basis in Fig. 2. Intense southerly winds would more effectively draw cool bottom water to the surface of the south basin than would gentle winds and thereby create a greater south–north temperature gradient.

Termination of the AHP in the Turkana basin is clearly reflected by an abrupt increase in the abundance of endogenic calcite in the south basin core at 5 ka (Halfman et al., 1994) and a dramatic shift to more salt-tolerant diatom species at 4.2 ka (Halfman et al., 1992) (Fig. 5). Eight piston cores from Lake Turkana were analyzed by Halfman et al. (1994) for abundance of calcite, which occurs primarily as euhedral crystals, 2–5 μm long in the laminated silty muds of the offshore basins (Halfman and Johnson, 1988). The abundance of endogenic calcite was interpreted to have been high during arid times when river input of silicate minerals was reduced and lake water salinity was elevated (Halfman et al., 1994). The history of carbonate deposition in the southern basin of the lake was considered by Halfman et al. (1994) to be the most reliable indicator of aridity in the region. The abrupt rise in carbonate abundance at ~5 ka nearly coincides with the youngest radiocarbon age on a raised beach terrace at the elevation of basin overflow to the Nile River and is compelling evidence for a shift at that time from open- to closed-basin conditions in the lake (Butzer, 1980; Owen et al., 1982). The fossil diatom record in core 2P in the south basin further documents the mid-Holocene shift to more arid conditions by 4.2 ka (Halfman et al., 1992). The diatom assemblage changes from dominance by low alkalinity (~1–2 meq/l) and conductivity (100–200 μS/cm) species, such as *Aulacoseira nyassensis* and *Stephanodiscus astraea*, to those that prefer more brackish conditions (alkalinity of ~5–10 meq/l and conductivity of about 400–2000 μS/cm), such as *Thalassiosira rudolfii* and *Surirella engleri*, indicating that salinity had risen and lake level had dropped substantially by this time (Gasse et al., 1983; Halfman et al., 1992) (Fig. 5).

Comparison of the thermal history of the south basin with the reconstructed history of aridity shows that the 8 centuries of warming leading up to the 5 ka thermal maximum occurred during the final millennium of the AHP (Fig. 5). The temperature decreased significantly from 5 ka until about 4 ka, as aridity became well established. Temperatures decreased gradually thereafter with superimposed centennial-scale variability. While this temperature reconstruction indicates that the thermal maximum occurred during the final millennium of the AHP, these phenomena do not share a similar temporal framework or causal mechanism, and as such, are not inherently related.

It is conceivable that when Lake Turkana was at a high stand and overflowing to the Nile during the AHP that the Thaumarchaeota present in the lake were different from the current community, and that the lacustrine calibration of Powers et al. (2010) might better capture LST at that time. If rising salinity caused a change in the lake Thaumarchaeotal community, then the temperature history for the lake might have been significantly different from that presented in Fig. 4. Any salinity change would not have occurred as soon as the lake level dropped from its outlet level. Rather, Yuretich and Cerling (1983) estimated that Lake Turkana salinity rose to its current value ~1420 years after basin closure, based on the chloride budget. If a shift in the Thaumarchaeota community happened ~4.2 ka when the diatom community changed abruptly, the 5 ka warming event would still stand out as a major thermal excursion in need of explanation, but may not represent the warmest part of the Holocene (Fig. 6). Alternatively, if the lack of anoxia in the deep water is the reason for the marine-like Thaumarchaeota community as we previously speculated, such a community shift at the time of falling lake level is not supported, for there is no evidence for deep-water anoxia in core 2P prior to 5 ka. There is no change in sedimentary structure (e.g., the presence of varves) or in the abundance of organic carbon across this boundary (Halfman, 2007). Consequently, we contend that there was little change in the Thaumarchaeotal community in Lake Turkana that would require a change in TEX_{86} calibration through this interval, though this shift cannot be fully ruled out.

4.2. Regional climate perspective

While the duration of the temperature record from Lake Turkana is only 6000 years, it calls attention to mid-Holocene warming present in longer temperature histories from other sites in tropical East Africa, suggesting a more regionally pervasive warming than previously highlighted. TEX_{86} temperature records from sediments of Lakes Malawi (Powers et al., 2005) and Tanganyika (Tierney et al., 2008), as well as a high resolution $\delta^{18}O$ record in an ice core from Mt. Kilimanjaro (Thompson et al., 2002), show mid-Holocene trends similar to those of Turkana (Fig. 7). Lake Malawi displays ~1.6 °C warming from 6 ka to a Holocene temperature maximum at 5 ka, followed by a cooling of

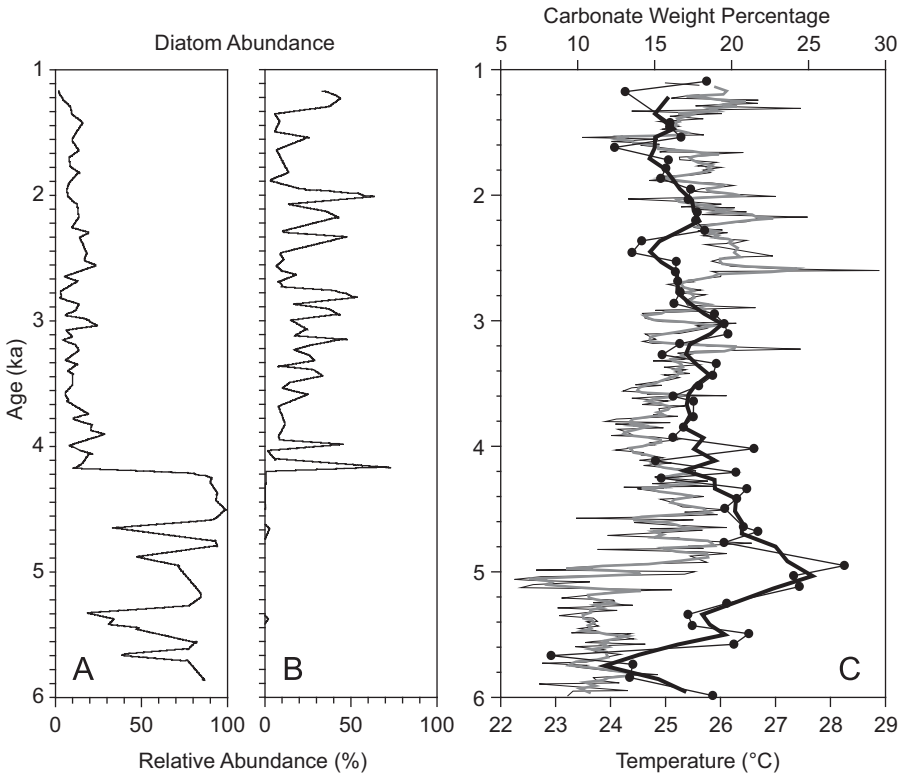

Fig. 5. Relative percentage of selected diatom genera abundances in core LT84-2P of (A) *Aulacoseira* and (B) *Thalassiosira* (Halfman et al., 1992). There is an abrupt shift in assemblage from freshwater diatom genera to more brackish-tolerant taxa ~4.2 ka. (C) Carbonate abundance as weight percent (depicted by fine line) (Halfman et al., 1994) and temperature (depicted by circles) in core LT84-2P with 3-point running averages shown in overlying heavy gray and black lines, respectively. A low abundance of carbonate has been previously interpreted as signifying a low alkalinity associated with humid intervals, leading to high lake levels, and vice versa (Halfman et al., 1994).

3 °C over the subsequent 2000 years (Fig. 7). Lake Tanganyika appears to have warmed by 1.3 °C over the millennium prior to a prolonged thermal maximum centered at 5.5–5 ka (Tierney et al., 2008). The lake then cooled gradually by about 2.5 °C over the following 2000 years (Fig. 7). This millennium of warmth at Tanganyika is also the warmest of the Holocene, with the exception of a brief excursion to warmer conditions at ~7 ka (Tierney et al., 2008). The mid-Holocene warming trends in Lakes Malawi and Tanganyika actually began at ~7 ka, and amounted to about 3.5 °C and 2.2 °C, respectively (Powers et al., 2005; Tierney et al., 2008; Woltering et al., 2011), and the details of the warming trends between 6 and 7 ka differ between the two lakes. Unfortunately the Turkana record does not extend further back than 6 ka, so we do not know if it, too, would have displayed the warming trend to have begun at 7 ka. The Kilimanjaro $\delta^{18}O$ record shows a positive shift of about 3‰ (Thompson et al., 2002) that is consistent with a warming trend of about 2 °C from about 6.5 to 4.5 ka, briefly interrupted by a shift to a light value at 5.2 ka. While Gasse (2002) speculated that this isotopic record was a reflection of precipitation amount and not temperature, recent oxygen isotopic data from diatoms in a core from Lake Challa, on the slope of Mt. Kilimanjaro, confirms the shift to have been due primarily to temperature (Barker et al., 2011). This isotopic enrichment is sustained for a few centuries, and is followed by a trend to lighter values from ~4.0 to 3.5 ka, reflecting a cooling as in Turkana (Fig. 7). However, the mid-Holocene Kilimanjaro isotope excursion is not unique; a ~2‰ shift to enriched values occurred earlier in the Holocene, between 9 and 7 ka (Thompson et al., 2002).

The 5 ka thermal excursion reported here is not expressed in a TEX_{86} record from Lake Victoria (Berke et al., 2011). We do not view this as evidence against the widespread warming at 5 ka that we report at four other sites in East Africa, but rather as an indication that there are exceptions to this trend, undoubtedly due to a spatially heterogeneous response to a forcing mechanism that is not yet well understood. Paleoclimate records from Lake Victoria (Johnson et al., 1998; Beuning et al., 2002) indicate that it also did not respond significantly to the Younger Dryas climate event, in stark contrast to other lakes in East Africa that experienced substantially drier and cooler conditions at that time (Talbot et al., 2007).

While the temperature records of Lakes Tanganyika and Malawi appear to be consistent with that of Turkana, the history of hydroclimate varies among these sites. The Tanganyika basin shows significant enrichment in δD of plant leaf waxes indicating a rapid shift to arid conditions shortly after the 5 ka thermal maximum at ~4.7 ka (Tierney et al., 2008), just like the Turkana basin. However, the Malawi basin, under Southern Hemisphere insolation forcing, responded differently with a relatively dry early Holocene (Finney et al., 1996) followed by wetter conditions after 8 ka, which lasted until about 1 ka, well beyond the termination of the AHP in the north (Castañeda et al., 2007). Thus, the onset of more arid conditions in equatorial East Africa at the end of the AHP was accompanied by significant cooling that extended well south of the equator to the Malawi basin, where there is no evidence for the existence of an early Holocene humid period.

In records from West Africa, the hydrologic history reconstructed using compound-specific δD from terrestrial leaf wax lipids preserved in a marine sediment core recovered off the mouth of the Congo River showed no significant change in hydrology in the Congo Basin at ~5 ka (Schefuß et al., 2005). Similarly, an air temperature history for this region based on tetraether compounds derived from soil bacteria preserved in the

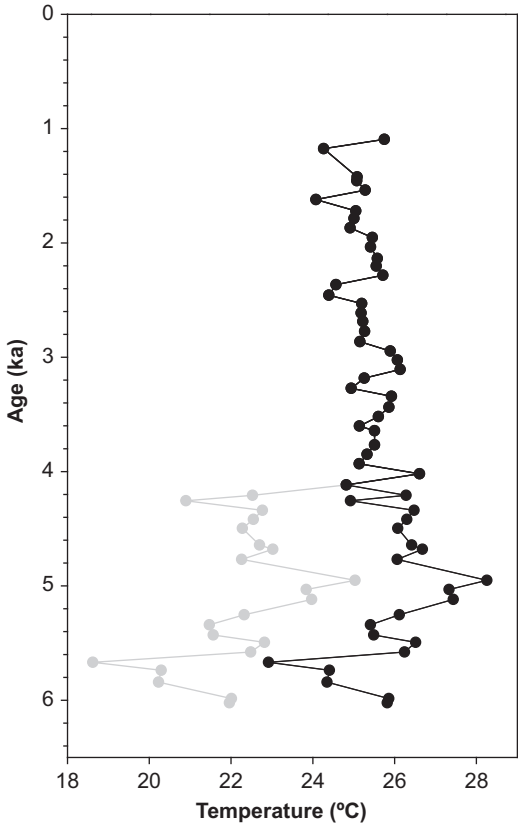

Fig. 6. Hypothetical thermal history from an inferred switch in Thaumarchaeota population, warranting a change from lacustrine (Powers et al., 2010) (in gray) to marine (Kim et al., 2010) (in black) calibration at ~4.2 ka. While this scenario cannot be ruled out, the significant thermal excursion at 5 ka described in Fig. 4 is still present, prior to any basin salinity changes.

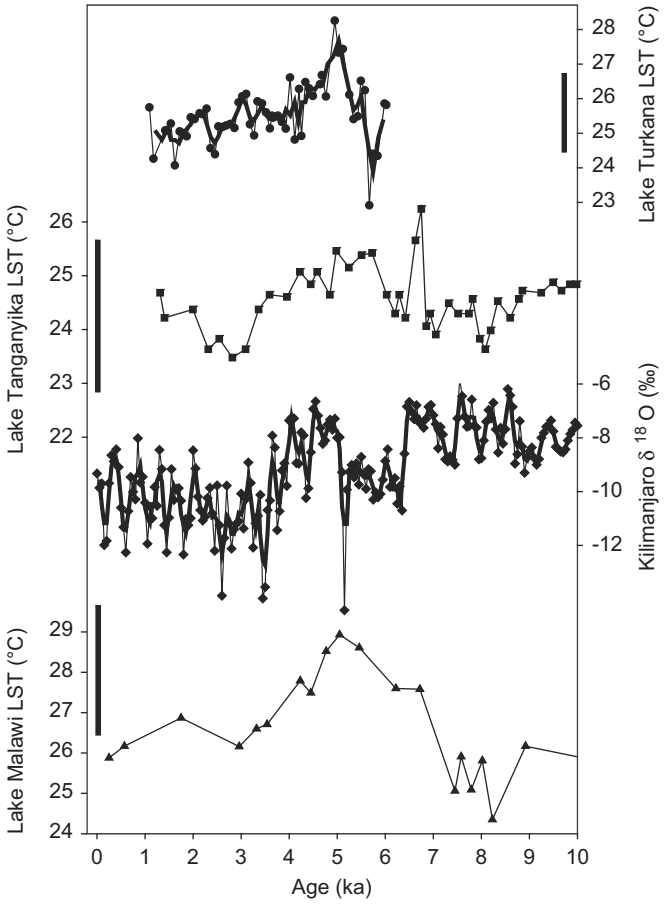

Fig. 7. Temperature variability in East Africa for the last 10,000 years, based on TEX_{86} lake surface temperatures from the south basin of Lake Turkana (circles), Lake Malawi (triangles), and Lake Tanganyika (squares), and the $\delta^{18}O$ record from an ice core from Mt. Kilimanjaro (diamonds). The solid bars on the left depict the temperature ranges observed in sediments from the last 200 years in Lake Turkana (cf. Fig. 8), Lake Tanganyika (Tierney et al., 2010a) and Lake Malawi (Powers et al., 2011).

same marine sediment core also displayed no significant temperature shift at 5 ka (Weijers et al., 2007).

4.3. The 5 ka thermal excursion in a modern climate context

To examine the long term TEX_{86} temperature record and 5 ka maximum from the perspective of modern climate we generated a high-resolution record of temperature in Lake Turkana spanning the last ~220 years from freeze-core LT94-14FC, taken from the south basin about 15 km northwest of core site LT84-2P (Fig. 1). The record displays decadal- to centennial-scale variability and ranges between ~24 °C and 27 °C (Fig. 8), an amplitude of change that is substantial, yet is observed as well in the un-smoothed temperature records of the two piston cores. Conditions appear cooler, on average, in the first half of the freeze-core record, corresponding to the so-called Little Ice Age, than after AD 1880. The last 50 years have been warmer on average than the previous 170 years, perhaps due to anthropogenic warming; however, the lake does not exhibit a simple, monotonic warming trend to the present day as is observed in Lake Tanganyika (Tierney et al., 2010a) and in Lake Malawi (Powers et al., 2011). Furthermore, unlike these two larger lakes to the south, Lake Turkana has not achieved temperatures in the past 50 years as warm as the thermal maximum at 5 ka (Fig. 7).

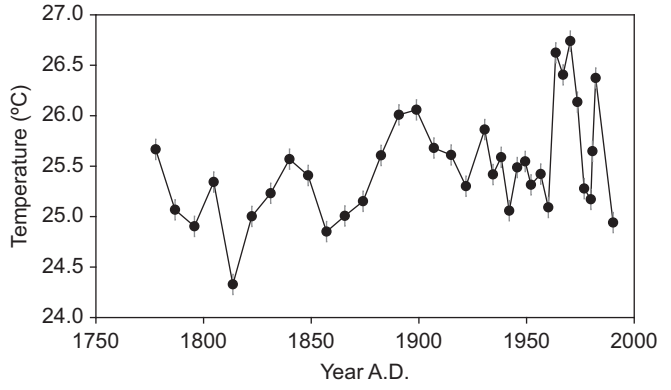

Fig. 8. TEX_{86} temperature reconstruction from freeze core LT94-14FC. Replicate analyses fell within ±0.2 °C but had an average difference of less than ±0.1 °C.

4.4. Possible forcing mechanism for a temperature excursion at the end of the AHP

The mid-Holocene experienced intermediate CO_2 and low CH_4 concentrations in the atmosphere, volcanic activity was relatively low but not anomalously quiescent, and solar radiative output was somewhat high but not exceptionally so (Mayewski et al., 2004).

Tierney et al. (2010b) noted the 5 ka warming of Lake Tanganyika and Lake Malawi and speculated that it may have resulted from the timing of peak local insolation. Lakes Tanganyika and Malawi undergo maximum evaporative cooling in June–August (JJA) under the influence of strong southerly winds

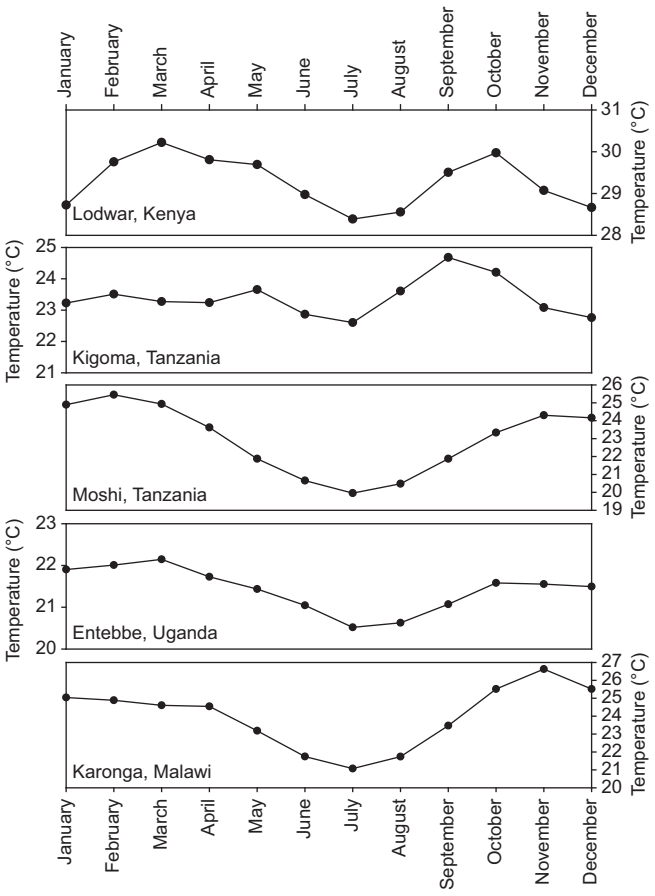

Fig. 9. Average monthly air temperatures near Lakes Tanganyika (Kigoma, Tanzania), Malawi (Karonga, Malawi), Victoria (Entebbe, Uganda), Turkana (Lodwar, Kenya) and Mt. Kilimanjaro (Moshi, Tanzania) based on available historical data (Lawrimore et al., 2011).

when the ITCZ is at its northern position over East Africa (Colter and Spigel, 1991). The winds subside as the ITCZ shifts southward in September–November (SON), the lakes warm, and thermal stratification is re-established (Eccles, 1974; Colter and Spigel, 1991). The warmest air temperatures in the Tanganyika and Malawi basins occur in September and November, respectively, when these lakes acquire most of their annual heat (Fig. 9). The timing of cooling and warming of Lake Turkana is quite similar to that of Lakes Malawi and Tanganyika (Hopson, 1982). Annual air temperatures at Moshi, Tanzania (near Mt. Kilimanjaro) and at Lodwar, Kenya (near Lake Turkana) peak in February–March of each year, with a second seasonal peak occurring in October–November (Lawrimore et al., 2011). Thus, the intensity of SON insolation may play an important role in the annual heat budgets of all four locations, and this peaked at 5 ka. By contrast, mean monthly temperature at Entebbe, Uganda (near Lake Victoria) remains nearly constant throughout the year, with an amplitude of seasonal air temperature range similar to Lodwar, Kenya, but with more subdued fall warming of less than 1 °C. This may be related to why insolation is no more important in SON than during any other month for Lake Victoria temperature, given its equatorial setting, and why Lake Victoria did not experience a thermal maximum at 5 ka (Berke et al., 2011).

If enhanced insolation in SON is offset by a comparable reduction in insolation in March-April-May (MAM), would we expect the mean annual temperature of the rift lakes to rise? The most important season to mean annual temperature may be the critical season of lake heating that follows the dry, windy months of JJA when maximum evaporative cooling occurred and the lakes are at their annual minimum temperature. The SON season is also unique, at least documented for Lakes Malawi and Tanganyika, as a time of major turbulence in the water column associated with internal waves generated by relaxation of the JJA wind forcing that tilted the thermocline downward from south to north (Eccles, 1974; Plisnier and Coenen, 2001). This redistribution of the longitudinal thermal structure would effectively mix warm surface water downward and enhance the net acquisition of heat by the lake. These dynamics are greatly subdued in MAM. Additionally, Verburg and Hecky (2003) demonstrated a strong correlation between warm season lake surface temperature and mean annual air temperature for Lake Tanganyika, for the period of record from 1963 to 1992, which suggests that the extent of warming during SON plays a significant role in annual mean temperature near these large East African lakes. At Mt. Kilimanjaro, the MAM long rains contribute the most to present annual precipitation, which has been attributed to interhemispheric differences in summer insolation (Verschuren et al., 2009). If true, SON short rains would have contributed more to the total annual precipitation at ~5 ka than today, and SON insolation would have had relatively more impact on the $\delta^{18}O$ signal.

Factors other than mean annual temperature may also impact TEX_{86} values, particularly those associated with the ecology of Thaumarchaeota. For example, water column depth or time of year that Thaumarchaeota are in greatest abundance may change through time, creating a temperature history that is influenced more by seasonality or habitat than by mean annual temperature. Little is known about potential seasonal bias in production and ultimately delivery of GDGTs to the sediments in these lakes, though the global linear regression of lacustrine TEX_{86} developed by Powers et al. (2010) shows the best statistical fit against mean annual lake surface temperature and not any mean seasonal temperatures, while studies of the global oceans have suggested possible seasonal influence in GDGT production (Herfort et al., 2006; Kim et al., 2010).

The timing and amplitude of the TEX_{86} shift that is independently observed near 5 ka in all three lakes is consistent, which suggests a common temperature history in the region rather than simultaneous ecological shifts unrelated to climate in these widely separated lakes. The intensity of upwelling may also affect lake surface water temperature, but it is unlikely to explain our observations. The range of temperature shift in Lake Turkana exceeds the vertical distribution of temperature in the present-day lake. Furthermore, upwelling is primarily developed at either end of a long, narrow rift lake. Our record from Turkana comes from the south end of the lake, the record from Malawi is from the north basin, and the TEX_{86} record of Tanganyika is from a central basin in the lake. No single shift in the regional wind field could account for a uniform swing in temperature in all three lakes, along with a comparable shift in isotopic composition of ice on Mt. Kilimanjaro.

While the paleotemperature records from Lakes Turkana, Malawi and Tanganyika all peak near 5 ka, the duration of this warm period may have been substantially longer in Malawi and Tanganyika than in Turkana (Fig. 6), and if so, the short duration of the warming in Turkana may be difficult to explain in terms of precession. Our record shows Turkana beginning to warm at just ~5.6 ka, when SON insolation was almost at maximum Holocene amplitude. The Turkana record does not extend back far enough to determine whether heating truly initiated so recently or whether it, too, may have begun to warm at about 7 ka, as did Tanganyika and Malawi. If this is not the case, we can only speculate that other factors that influence the mean annual temperature of Lake Turkana subdued the influence of SON

insolation until a threshold was surpassed at ~5.6 ka, allowing the lake to respond finally to this critical seasonal forcing.

5. Conclusions

We report a significant temperature shift that accompanied the end of the AHP in tropical East Africa. The maximum temperatures achieved at 5 ka were nearly as warm as current temperatures in Lakes Tanganyika and Malawi and exceeded the temperature of modern Lake Turkana after a century of significant warming possibly due to anthropogenic impact. We attribute this temperature excursion to September–November insolation, which peaked at 5 ka and is the season of near-maximum air temperature throughout the region when the rift lakes warm considerably. The profound change in temperature that accompanied the shift to widespread aridity undoubtedly contributed to a migration of many species, including our human ancestors, through tropical East Africa and the Sahara, retreating from increasingly inhospitable conditions to more favorable landscapes. Further investigation of the ecological impact of this mid-Holocene thermal excursion may provide insight into the potential influence of future warming in the region, where a rapidly expanding human population is particularly vulnerable to the impact of climate on agriculture and fisheries.

Acknowledgments

We thank LacCore, the National Repository for Lake Sediment Cores at the University of Minnesota for core access and assistance. E.T. Brown, S. Colman, and Z. Liu provided useful comments on an earlier version of the manuscript. We thank Ellen Hopmans, Jort Ossebaar, Sarah Grosshuesch, Julia Halbur, and Doug Klotter for laboratory assistance. This research was funded by Grant NA-060-AR4310113 from the U.S. Department of Commerce, National Oceanic and Atmospheric Administration. Support from the Gledden Fellowship to J.P.W. is acknowledged. Work prepared while J.P.W. on leave at the Center for Water Research, University of Western Australia and the WA-Organic & Isotope Geochemistry Center, Curtin University of Technology. This work forms contribution 2402-JW at the Center for Water Research, The University of Western Australia.

Appendix A. Supplementary materials

Supplementary data associated with this article can be found in the online version at http://dx.doi.org/10.1016/j.epsl.2012.07.008.

References

Barker, P.A., Hurrell, E.R., Leng, M.J., Wolff, C., Cocquyt, C., Sloane, H.J., Verschuren, D., 2011. Seasonality in equatorial climate over the past 25 kyr revealed by oxygen isotope records from Mount Kilimanjaro. Geology 39, 1111–1114.

Berke, M.A., 2011. Molecular and Isotopic Records of Climate Variability and Vegetation Response in Tropical East Africa During the Late Pleistocene and Holocene. Ph.D. Dissertation, University of Minnesota.

Beuning, K., Kelts, K., Russell, J., Wolfe, B.B., 2002. Reassessment of Lake Victoria—upper Nile River paleohydrology from oxygen isotope records of lake-sediment cellulose. Geology 30, 559–562.

Blaga, C., Reichart, G.-J., Heiri, O., Sinninghe Damsté, J., 2009. Tetraether membrane lipid distributions in water-column particulate matter and sediments: a study of 47 European lakes along a north–south transect. J. Paleolimnol. 41, 523–540.

Blaga, C.I., Reichart, G.-J., Vissers, E.W., Lotter, A.F., Anselmetti, F.S., Sinninghe Damsté, J.S., 2011. Seasonal changes in glycerol dialkyl glycerol tetraether concentrations and fluxes in a perialpine lake: implications for the use of the TEX_{86} and BIT proxies. Geochim. Cosmochim. Acta 75, 6416–6428.

Brochier-Armanet, C., Boussau, B., Gribaldo, S., Forterre, P., 2008. Mesophilic crenarchaeota: proposal for a third archaeal phylum, the Thaumarchaeota. Nat. Rev. Microbiol. 6, 245–252.

Butzer, K.W., 1980. The Holocene lake plain of north Rudolph, East Africa. Phys. Geogr. 1, 42–58.

Castañeda, I.S., Werne, J., Johnson, T.C., 2007. Wet and arid phases in the southeast African tropics since the Last Glacial Maximum. Geology 35, 823–826.

Cerling, T.E., 1979. Paleochemistry of Plio-Pleistocene Lake Turkana, Kenya. Palaeogeogr. Palaeoclimatol. Palaeoecol. 27, 247–285.

Claussen, M., Gayler, V., 1997. The greening of the Sahara during the mid-Holocene: results of an interactive atmosphere-biome model. Global Ecol. Biogeogr. 6, 369–377.

Colter, G.W., Spigel, R.H., 1991. Hydrodynamics. In: Colter, G.W. (Ed.), Lake Tanganyika and Its Life. Oxford University Press, London, pp. 47–75.

deMenocal, P., Ortiz, J., Guilderson, T., Adkins, J., Sarnthein, M., Baker, L., Yarusinsky, M., 2000. Abrupt onset and termination of the African Humid Period: rapid climate responses to gradual insolation forcing. Quat. Sci. Rev. 19, 347–361.

Eccles, D.H., 1974. An outline of the physical limnology of Lake Malawi (Lake Nyasa). Limnol. Oceanogr. 19, 730–742.

Ferguson, A.J.D., Harbott, B.J., 1982. Geographical, physical and chemical aspects of Lake Turkana, in: Hopson, A.J. (Ed.), Lake Turkana: A Report on the Findings of the Lake Turkana Project, 1972–1975. Overseas Development Administration, London, pp. 1–108.

Finney, B.P., Scholz, C.A., Johnson, T.C., Trumbore, C., 1996. Late Quaternary lake-level changes of Lake Malawi. In: Johnson, T.C., Odada, E.O. (Eds.), The Limnology, Climatology, and Paleoclimatology of the East African Rift Lakes. Gordon and Breach, Amsterdam, pp. 495–508.

Gasse, F., 2002. Kilimanjaro's Secrets Revealed. Science 298, 548–549.

Gasse, F., Talling, J.F., Kilham, P., 1983. Diatom assemblages in East Africa: classification, distribution and ecology. Rev. D'Hydrobiol. Trop. 16, 3–34.

Halfman, J.D., 2007. High-resolution sedimentology and paleoclimatology of Lake Turkana, Kenya, Geology. Duke University, Durham (p. 188).

Halfman, J.D., Jacobson, D.F., Cannella, C.M., Haberyan, K.A., Finney, B.P., 1992. Fossil diatoms and the mid to late Holocene paleolimnology of Lake Turkana, Kenya: a reconaissance study. J. Paleolimnol. 7, 23–35.

Halfman, J.D., Johnson, T.C., 1988. High-resolution record of cyclic climatic change during the past 4 ka from Lake Turkana, Kenya. Geology 16, 496–500.

Halfman, J.D., Johnson, T.C., Finney, B.P., 1994. New AMS dates, stratigraphic correlations and decadal climatic cycles for the past 4 ka at Lake Turkana, Kenya. Palaeogeogr. Palaeoclimatol. Palaeoecol. 111, 83–98.

Herfort, L., Schouten, S., Boon, J.P., Sinninghe Damsté, J.S., 2006. Application of the TEX_{86} temperature proxy in the southern North Sea. Org. Geochem. 37, 1715–1726.

Hopmans, E.C., Schouten, S., Pancost, R.D., van der Meer, M.T.J., Sinninghe Damsté, J.S., 2000. Analysis of intact tetraether lipids in archaeal cell material and sediments by high-performance liquid chromatography/atmospheric-pressure-chemical-ionization mass spectrometry. Rapid Commun. Mass Spectrom. 14, 585–589.

Hopmans, E.C., Weijers, J.W.H., Schefuß, E., Herfort, L., Sinninghe Damsté, J.S., 2004. A novel proxy for terrestrial organic matter in sediments based on branched and isoprenoid tetraether lipids. Earth Planet. Sci. Lett. 224, 107–116.

Hopson, A.J., 1982. Lake Turkana: A Report on the Findings of the Lake Turkana Project, 1972–1975. Overseas Development Administration, London.

Huguet, C., Hopmans, E.C., Febo-Ayala, W., Thompson, D.H., Sinninghe Damsté, J.S., Schouten, S., 2006. An improved method to determine the absolute abundance of glycerol dibiphytanyl glycerol tetraether lipids. Org. Geochem. 37, 1036–1041.

Johnson, T.C., Chan, Y., Beuning, K.R.M., Kelts, K., Ngobi, G., Verschuren, D., 1998. Biogenic silica profiles in Holocene cores from Lake Victoria: implications for lake level history and initation of the Victoria Nile. In: Lehman, J.T. (Ed.), Environmental Change and Response in East African Lakes. Kluwer Academic Publishers, Dordrecht, Germany, pp. 75–88.

Kim, J.-H., van der Meer, J., Schouten, S., Helmke, P., Willmott, V., Sangiorgi, F., Koç, N., Hopmans, E.C., Sinninghe Damsté, J.S., 2010. New indices and calibrations derived from the distribution of crenarchaeal isoprenoid tetraether lipids: implications for past sea surface temperature reconstructions. Geochim. Cosmochim. Acta 74, 4639–4654.

Konneke, M., Bernhard, A.E., de la Torre, J.R., Walker, C.B., Waterbury, J.B., Stahl, D.A., 2005. Isolation of an autotrophic ammonia-oxidizing marine archaeon. Nature 437, 543–546.

Kuper, R., Kropelin, S., 2006. Climate-controlled Holocene occupation in the Sahara: motor of Africa's evolution. Science 313, 803–807.

Kutzbach, J.E., Street-Perrott, F.A., 1985. Milankovitch forcing of fluctuations in the level of tropical lakes from 18 to 0 k yr BP. Nature 317, 130–134.

Lawrimore, J.H., Menne, M.J., Gleason, B.E., Wuertz, D.B., Williams, C.N., Vose, R.S., Rennie, J., 2011. An overview of the Global Historical Climatology Network monthly mean temperature data set, version 3. J. Geophys. Res. 116, D19121 (doi: 19110.11029/12011JD016187).

Liu, Z., Wang, Y., Gallimore, R., Gasse, F., Johnson, T., deMenocal, P., Adkins, J., Notaro, M., Prentice, I.C., Kutzbach, J., Jacob, R., Behling, P., Wang, L., Ong, E., 2007. Simulating the transient evolution and abrupt change of Northern Africa atmosphere–ocean–terrestrial ecosystem in the Holocene. Quat. Sci. Rev. 26, 1818–1837.

Mayewski, P.A., Rohling, E.E., Stager, J.C., Karlen, W., Maasch, K.A., Meeker, L.D., Meyerson, E.A., Gasse, F., can Kreveld, S., Holmgren, K., Lee-Thorp, J., Rosqvist,

G., Rack, F., Staubwasse, M., Schneider, R.R., Steig, E.J., 2004. Holocene climate variability. Quat. Res. 62, 243–255.
Nicholson, S.E., Kim, J., Hoopingarner, J., 1988. Atlas of African rainfall and its interannual variability. Department of Meteorology, Florida State University, Tallahassee (p. 237).
Niedermeyer, E.M., Schefuß, E., Sessions, A.L., Mulitza, S., Mollenhauer, G., Schulz, M., Wefer, G., 2010. Orbital- and millennial-scale changes in the hydrologic cycle and vegetation in the western African Sahel: insights from individual plant wax δD and δ^{13}C. Quat. Sci. Rev. 29, 2996–3005.
Owen, R.B., Barthelme, J.W., Renaut, R.W., Vincens, A., 1982. Paleolimnology and archaeology of Holocene deposits north-east of Lake Turkana, Kenya. Nature 298, 523–529.
Pitcher, A., Hopmans, E.C., Mosier, A.C., Park, S.-J., Rhee, S.-K., Francis, C.A., Schouten, S., Sinninghe Damsté, J.S., 2011. Core and intact polar glycerol dibiphytanyl glycerol tetraether lipids of ammonia-oxidizing Archaea enriched from marine and estuarine sediments. Appl. Environ. Microbiol. 77, 3468–3477.
Plisnier, P.-D., Coenen, E.J., 2001. Pulsed and dampened annual limnological fluctuations in Lake Tanganyika. In: Munawar, M., Hecky, R.E. (Eds.), The Great Lakes of the World (GLOW): Food-Web, Health and Integrity. Backhuys Publishers, Leiden, pp. 83–96.
Powers, L.A., Johnson, T.C., Werne, J.P., Castañeda, I., Hopmans, E.C., Sinninghe Damsté, J.S., Schouten, S., 2005. Large temperature variability in the southern African tropics since the Last Glacial Maximum. Geophys. Res. Lett. 32, L08706 (doi: 08710.01029/02004GL022014).
Powers, L.A., Johnson, T.C., Werne, J.P., Castañeda, I., Hopmans, E.C., Sinninghe Damsté, J.S., Schouten, S., 2011. Organic geochemical records of environmental variability in Lake Malawi during the last 700 years, Part I: the TEX_{86} temperature record. Palaeogeogr. Palaeoclimatol. Palaeoecol. 303, 133–139.
Powers, L.A., Werne, J.P., Johnson, T.C., Hopmans, E.C., Sinninghe Damsté, J.S., Schouten, S., 2004. Crenarchaeotal membrane lipids in lake sediments: a new paleotemperature proxy for continental paleoclimate reconstruction? Geology 32, 613–616.
Powers, L.A., Werne, J.P., Van der woude, A.J., Sinninghe Damsté, J.S., Hopmans, E.C., Schouten, S., 2010. Applicability and calibration of the TEX_{86} paleothermometer in lakes. Org. Geochem. 41, 404–413.
Reimer, P.J., Baillie, M.G.L., Bard, E., Bayliss, A., Beck, J.W., Blackwell, P.G., C., B.R., Buck, C.E., Burr, G.S., Edwards, R.L., Friedrich, M., Grootes, P.M., Guilderson, T.P., Hajdas, I., Heaton, T.J., Hogg, A.G., Hughen, K.A., Kaiser, K.F., Kromer, B., McCormac, F.G., Manning, S.W., Reimer, R.W., Richards, D.A., Southon, J.R., Talamo, S., Turney, C.S.M., van der Plicht, J., Weyhenmeyer, C.E., 2009. IntCal09 and Marine09 radiocarbon age and calibration curves, 0–50,000 years Cal BP. Radiocarbon 51, 1111–1150.
Ricketts, R.D., Anderson, R.F., 1998. A direct comparison between the historical record of lake level and the δ^{18}O signal in carbonate sediments from Lake Turkana, Kenya. Limnol. Oceanogr. 43, 811–822.
Schefuß, E., Schouten, S., Schneider, R.R., Sinninghe Damsté, J.S., 2005. Central African hydrologic changes during the past 20,000 years. Nature 437, 1003–1006.
Schouten, S., Hopmans, E.C., Schefuß, E., Sinninghe Damsté, J.S., 2002. Distributional variations in marine crenarchaeotal membrane lipids: a new tool for reconstructing ancient sea water temperatures? Earth Planet. Sci. Lett. 204, 265–274.
Schouten, S., Huguet, C., Hopmans, E.C., Kienhuis, M.V.M., Sinninghe Damsté, J.S., 2007a. Analytical methodology for TEX_{86} paleothermometry by high-performance liquid chromatography/atmospheric pressure chemical ionization-mass spectrometry. Anal. Chem. 79, 2940–2944.
Schouten, S., M.T.J., v.d.M., E., H., W.I., R., Reysenbach, A.-L., Ward, D.M., Sinninghe Damsté, J.S., 2007b. Archaeal and bacterial glycerol dialkyl glycerol tetraether lipids in hot springs of Yellowstone National Park. Appl. Environ. Microbiol. (73), 6181–6191.
Sinninghe Damsté, J.S., Hopmans, E.C., Schouten, S., van Duin, A.C.T., Geenevasen, J.A.J., 2002. Crenarchaeol: the characteristic core glycerol dibiphytanyl glycerol tetraether membrane lipid of cosmopolitan pelagic crenarchaeota. J. Lipid Res. 43, 1641–1651.
Talbot, M.R., Filippi, M.L., Jensen, N.B., Tiercelin, J.-J., 2007. An abrupt change in the African monsoon at the end of the Younger Dryas. Geochem. Geophys. Geosyst. 8, Q03005.
Thompson, L.G., Mosley-Thompson, E., Davis, M.E., Henderson, K.A., Brecher, H.H., Zagorodnov, V.S., Mashiotta, T.A., Lin, P.-N., Mikhalenko, V.N., Hardy, D.R., Beer, J., 2002. Kilimanjaro ice core records: evidence of Holocene climate change in tropical Africa. Science 298, 589–593.
Tierney, J.E., Lewis, S.C., Cook, B.I., LeGrande, A.N., Schmidt, G.A., 2011. Model, proxy and isotopic perspectives on the East African Humid Period. Earth Planet. Sci. Lett. 307, 103–112.
Tierney, J.E., Mayes, M.T., Meyer, N., Johnson, C., Swarzenski, P.W., Cohen, A.S., Russell, J.M., 2010a. Late twentieth-century warming in Lake Tanganiyika unprecedented since AD 500. Nat. Geosci. 3, 422–425.
Tierney, J.E., Russell, J.M., Huang, Y., Sinninghe Damsté, J.S., Hopmans, E.C., Cohen, A.S., 2008. Northern Hemisphere controls on tropical southeast African climate during the past 60,000 years. Science 322, 252–255.
Tierney, J.E., Russell, J.M., Huang, Y.S., 2010b. A molecular perspective on Late Quaternary climate and vegetation change in the Lake Tanganyika basin, East Africa. Quat. Sci. Rev. 29, 787–800.
Verburg, P., Hecky, R.E., 2003. Wind patterns, evaporation, and related physical variables in Lake Tanganyika, East Africa. J. Great Lakes Res. 29, 48–61.
Verschuren, D., Sinninghe Damste, J.S., Moernaut, J., Kristen, I., Blaauw, M., Fagot, M., Haug, G.H., 2009. Half-precessional dynamics of monsoon rainfall near the East African Equator. Nature 462, 637–641.
Vincens, A., Buchet, G., Servant, M., collaborators, E., 2010. Vegetation response to the ''African Humid Period'' in central Cameroon (7°N)—new pollen insight from Lake Mbalang. Clim. Past 6, 281–294.
Weijers, J.W.H., Schefuß, E., Schouten, S., Sinninghe Damsté, J.S., 2007. Coupled thermal and hydrological evolution of tropical Africa over the last deglaciation. Science 315, 1701–1704.
Weninger, B., Jöris, O., Danzeglocke, U., 2011. CalPal-2007. 〈http://www.calpal-online.de/〉.
Woltering, M., Johnson, T.C., Werne, J.P., Schouten, S., Sinninghe Damsté, J.S., 2011. Late Pleistocene temperature history of Southeast Africa: a TEX_{86} temperature record from Lake Malawi. Palaeogeogr. Palaeoclimatol. Palaeoecol. 303, 93–102.
Wuchter, C., Abbas, B., Coolen, M.J.L., Herfort, L., van Bleijswijk, J., Timmers, P., Strous, M., Teira, E., Herndl, G.J., Middelburg, J.J., Schouten, S., Sinninghe Damsté, J.S., 2006. Archaeal nitrification in the ocean. Proc. Natl. Acad. Sci. 103, 12317–12322.
Wuchter, C., Schouten, S., Coolen, M.J.L., Sinninghe Damsté, J.S., 2004. Temperature-dependent variation in the distribution of tetraether membrane lipids of marine Crenarchaeota: implications for TEX_{86} paleothermometry. Paleoceanography, 19, http://dx.doi.org/10.1029/2004PA001041.
Yuretich, R.F., Cerling, T.E., 1983. Hydrogeochemistry of Lake Turkana, Kenya: mass balance and mineral reactions in an alkaline lake. Geochim. Cosmochim. Acta 47, 1099–1109.